ChemComm

Accepted Manuscript

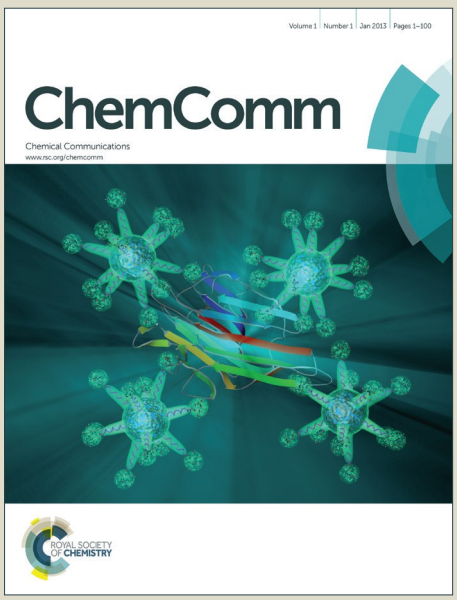

ROYAL SOCIETY OF CHEMISTRY

www.rsc.org/chemcomm

ChemComm

COMMUNICATION

A new chiral boron cluster B_{44} containing nonagonal holes

Truong Ba Tai[a,b,*] and Minh Tho Nguyen[b,*]

Received 00th January 20xx,
Accepted 00th January 20xx

DOI: 10.1039/x0xx00000x

www.rsc.org/

The B_{44} has a cage-like structure containing two hexagonal, two heptagonal and two nonagonal holes. The presence of nonagonal holes is a new and remarkable finding since they have never been reported before for clusters. The present work does not only identify the new chiral members, but also provides more insight into the growth motif of large-sized boron clusters.

Stimulated by the beautiful geometrical structure and unique properties of the carbon fullerene C_{60},[1] a large number of theoretical and experimental studies have been carried out during many past decades with the aim of finding similar caged structures of other elements. As a neighbour of carbon in the Periodic Table, it is expected that boron atoms can also aggregate to form all-boron fullerenes. The boron buckyball B_{80}, an isoelectronic species of fullerene C_{60}, was proposed in 2007 by Yakobson and coworkers.[2] Subsequently, many theoretical investigations on boron fullerenes and their derivatives were carried out,[3] in spite of the fact that such structure have not observed in the experiment yet.[4]

Recently, the B_{40} cluster has been discovered to exist as an all-boron fullerene containing four heptagonal holes and two hexagonal holes.[5] The dynamical behaviour of this species was further analyzed.[6] Some other cage-like structures were more recently reported. The fullerene B_{38} containing four hexagonal holes was found as the lowest-lying isomer, which is almost degenerate in energy with a quasi-planar structure.[7] The B_{39}^- anion was reported to exhibit a chiral cage-like structure containing three heptagonal holes and three hexagonal holes.[8] More recently, Zhai *et al.*[9] found that the monocation B_{41}^+ and dication B_{42}^{2+} have similar geometrical cage structures, even though the neutral B_{42} has a triple ring tubular shape in its ground state.[5a]

A common motif of these cages is that each of them contains both hexagonal B_7 and heptagonal B_6 holes. The B_{41}^+ and B_{42}^{2+} cations are constructed by replacing one and two hexagonal B_6 holes of B_{40} by the heptagonal B_7 holes, respectively. It is worthy to note that the quasi-planar and convex structures containing pentagonal, hexagonal and heptagonal holes were observed at smaller-sized boron clusters such as B_{30},[10] B_{32}[11] and B_{36}.[12] Two smallest three-dimensional structures were found at B_{14}[13] and B_{28}.[14] An intriguing question emerges as to whether and how cage-like structures exist in large-sized boron clusters.

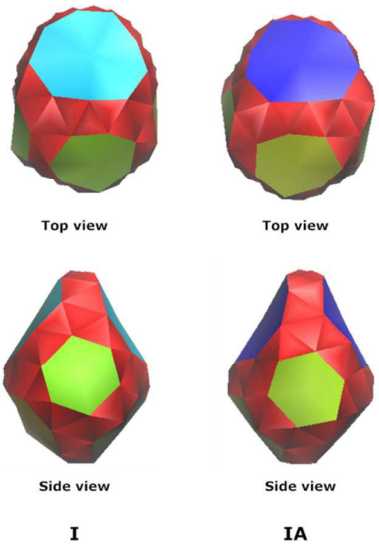

Fig. 1 Shape of the global energy minimum structure **I** of B_{44} and its enantiomer **IA**

Based on theoretical results obtained from the first-principles calculations, we found that the boron cluster B_{44} also exhibits chiral cage-like structures. More interestingly, its most stable form contains two nonagonal B_9 holes which have never been observed before for boron clusters, or even for clusters of other elements. The structure of this B_{44} cluster is displayed in Fig. 1. These predictions do not only identify a new chiral member of boron clusters, but they also give us

[a] *Computational Chemistry Research Group & Faculty of Applied Sciences, Ton Duc Thang University, Ho Chi Minh City, Vietnam*
[b] *Department of Chemistry, KU Leuven, Leuven City, Belgium*
Emails: truongbatai@tdt.edu.vn; truong.batai@chem.kuleuven.be; minh nguyen@chem.kuleuven.be
Electronic Supplementary Information (ESI) available: See DOI: 10.1039/x0xx00000x

more insight into the growth motif of larger size boron clusters.

Extensive structural searches were carried out by using stochastic random searching procedures,[15] and manual structural construction based on the known structures of smaller sized boron clusters. Low-lying isomers B_{44} with relative energy of 0.0 - 5.0 eV obtained from initial geometry optimizations at the PBE0/3-21G were fully optimized at higher level of theory PBE0/6-311+G(d).[16] To identify a true global minimum, single-point electronic energies of a few lowest-lying B_{44} isomers were subsequently calculated using the couple-cluster theory CCSD(T)/6-31G(d) method[17] at their PBE0/6-311+G(d) optimized geometries. These computational methods were effectively used to establish the energy landscape of boron clusters in the literature. All calculations were performed using the Gaussian 09[18] and Molpro 2012 packages.[19]

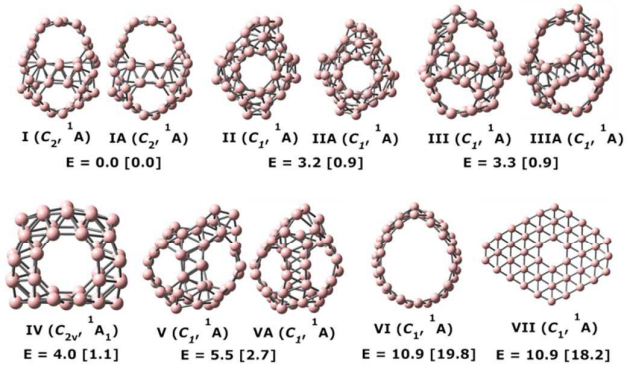

Fig. 2 Optimized geometries and relative energies (kcal.mol^{-1}) of the lowest-lying isomers B_{44} obtained at the PBE0/6-311+G(d) level (values in square brackets are obtained at CCSD(T)/6-31G(d))

The optimized geometries and relative energies (kcal.mol^{-1}) of few lowest-lying B_{44} isomers are depicted in Fig. 2, while those of less stable isomers are shown in Figure S1 of the Supplementary Information. At the first glance, it can be seen that almost lowest-lying isomers are three-dimensional structures. At the PBE0/6-311+G(d) level, our calculations show that the structure **I** (and its degenerate enantiomer **IA**) is the most stable form. This structure is composed of 52 triangular units and six polygonal holes. The latter includes two nonagonal B_9, two heptagonal B_7 and two hexagonal B_6 holes. It can be constructed by replacing two neighboured heptagonal B_7 holes of the B_{40} fullerene by two nonagonal B_9 holes. Similar to the cage-like boron structures B_n,[5,8,9] the B_{44}-**I** follows the Euler's rule for a polyhedron: V(*100* edges) = F(*52* triangular + *2* hexagonal + *2* heptagonal + *2* nonagonal faces) + V(*44* vertices) - *2*.

Three cage-like structures, namely **II**, **III** and **IV**, are the next isomers with relative energies of 3 - 6 kcal.mol^{-1} higher than the lost stable **I**. Similar to the bonding motif of the isomer **I**, the isomer **II** (and its enantiomer **IIA**) can be constructed by replacing two neighboured heptagonal B_7 holes in B_{40} by two octagonal B_8 holes. The isomer **III** (and its enantiomer **IIIA**) is formed by replacing two neighboured hexagonal B_6 holes in B_{39}^- by two octagonal B_8 holes. Both isomers are almost degenerate in energy as computed at both levels of theory DFT and CCSD(T). The isomer **IV** contains two octagonal B_8, two heptagonal B_7 and one hexagonal B_6 holes. A double-ring form **VI** and quasi-planar containing six-membered B_6 hole **VII** are located at 11 kcal.mol^{-1} higher in energy as compared to the global minimum **I**. In a previous report, Wang et al.[20] identified the B_{44} as an irregular cage containing one five-membered, five six-membered and two seven-membered rings. However, our PBE0 results showed that this structure is 11.4 kcal.mol^{-1} less stable than the isomer **I**.

Our CCSD(T) results show the same energy ordering that the isomer **I** is the most stable isomer for B_{44}. However, the energy gaps between **I** and isomers **II**, **III and IV** become closer. Four structures **I**, **II**, **III** and **IV** are nearly degenerate with energy gap of ~1 kcal.mol^{-1}. The isomer **V** is somewhat less stable than **I** with a relative energy of 3 Kcal.mol^{-1}. Two structures, including the double ring form **VI** and the quasi-planar form **VII**, are found much less stable, and are at 18 and 20 kcal.mol^{-1} higher in energy as compared to **I**, respectively. It is in agreement with the earlier reports that the PBE0 functional tends to overestimate the energy of the tubular and quasi-planar forms.[8,9,21,22] Although the CCSD(T) method somewhat favours cage-like structures, the large differences in energy between the cages **I**-**V** and other forms such as **VI** and **VII** lend support for the finding that the **I** is the most stable form of B_{44}. In addition, we would expect that the four isomers **I**-**V** will be appeared in experimental observations since their energies are close to each other.

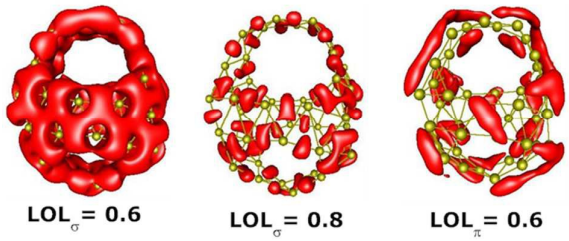

Fig. 3 Plots of LOL$_\sigma$ and LOL$_\pi$ for isomer **I** (C_2, ^{1}A)

To probe more understanding about the stability of isomers B_{44}, we also performed molecular dynamic (MD) simulations for the four lowest-lying isomers **I** - **IV** by using the CP2K programs.[23] The simulations were carried out at temperatures of 300 and 500K during a time of 30 ps. The PBE functional was used in conjunction with the 6-31G(d) basis set. The RMSD values were calculated using VMD code[24] and their plots were depicted in Figure S2 (SI) together with the movies of simulation trajectories at 500 K (SI). During the BO-MD simulations at 300 and 500K, the isomer **I** retains its connectivity pattern and cage-like shape with two nonagonal holes. As discussed above, the isomers **II** and **III** are located on the energy landscape of B_{44} with tiny differences in relative energy. Our simulations showed that there is a continuous transformation between one hexagonal hole of **II** and one heptagonal hole of **III** at both temperatures of 300 and 500 K. Although the isomer **IV** has low relative energy, it is much

kinetically less stable. The connectivity pattern of **IV** is broken after a simulation time of 0.1 ps at 500 K, and 0.5 ps at 300 K. The isomer **V** shows more kinetic stability as it still maintains its original pattern during the simulation time at both temperatures mentioned above.

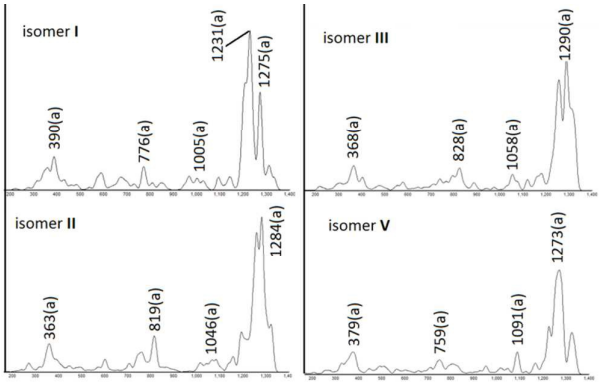

Fig. 4. Simulated infrared spectra of the lowest-lying B_{44} isomers.

The characteristics of electron delocalization and aromaticity of boron clusters have attracted much attention from the view of theory.[25,26] To gain more insight into the higher stability of the isomer **I**, its bonding pattern is now examined by using the topological analysis of localized orbital locator (LOL)[27] that is based on a comparison of the local non-interacting kinetic energy density with that of the uniform electron gas. This approach was effectively applied to analyze chemical bonding and electron delocalization of many types of molecules in the earlier studies.[28,29] The picture of canonical molecular orbitals (CMOs) of **I** shows that it contains a total of 66 valence MOs which are separated into 52 σ-MOs and 14 π-MOs. The LOL of σ electron systems (LOL_σ) for **I** at values 0.6 and 0.8 displayed in Fig. 3 point out that there is excellent electron delocalization over the whole structure. At the value of 0.8, the isosurface of LOL_σ is separated into 52 basins that contribute to the σ chemical bonds of 52 triangular units of the structure. Similarly, the LOL of π-electron system (LOL_π) at value of 0.6 of B_{44}-**I** also shows a good π electron delocalization. Electrons are distributed on the skeleton of each 9-membered ring. Overall, electron distribution forms two highly delocalized σ and π bonding systems, and consequently make the isomer **I** highly stable and aromatic.

The nucleus independent chemical shift (NICS) can effectively be used to evaluate the aromatic feature.[30] Our NICS calculations at the central positions of above caged-like structures showed that all these cages exhibit high aromaticity. The NICS value of -21 is obtained at the center of cage **I** which is comparable to the NICS values obtained for boron cages, e.g. -22 for B_{32}[20] and -38 for B_{28}.[14] Although being less stable than the isomer **I**, the structures **II** – **V** even possess more negative NICS values (NICS(**II**) = 28, NICS(**III**) = -28, NICS (**IV**) = -32 and NICS(**V**) = -33). It seems that the presence of large nine-membered rings somewhat decreases aromaticity of **I** as compared to other isomers.

To provide with a support for future experimental studies, simulations of infrared (IR) spectra of four stable lowest-lying isomers **I**, **II**, **III** and **V**, which are obtained at the PBE0/6-311+G(d) level are depicted in Fig. 4. All isomers have similar spectral features with high intensity peaks located close to each other. The spectrum of **I** shows five major peaks centered at 390, 776, 1005, 1231 and 1275 cm^{-1}. These peaks are approximate to the intense peaks of 380, 713 and 1274 cm^{-1} of the boron buckyball B_{40}.9

Conclusions

We performed a theoretical study on the B_{44} cluster by using both DFT and CCSD(T) methods. We found that the most stable form of B_{44} is cage-like structure **I** containing two nonagonal, two heptagonal and two hexagonal holes. The presence of nonagonal holes is remarkably interesting since it has never been observed before for boron clusters (and probably for other elemental clusters). The structure is composed of two delocalized σ and π bonding systems that confer a high stability to **I**. BO-MD simulations of **I** at both 300 and 500 K showed both thermodynamic and kinetic stabilities. These predictions do not only establish a new chiral member of boron clusters, but they also give us additional insight into the growth motif of boron clusters. The unprecedented presence of nonagonal holes in a boron cluster of medium size suggests that new structural features for larger size aggregates are still to be discovered.

We are indebted to the KU Leuven Research Council (GOA program) and Vlaams Supercomputer Centrum (VSC). TBT thanks the FWO-Vlaanderen for a postdoctoral fellowship.

Notes and references

1 H. W. Kroto, J. R. Heath, S. C. O'Brien, R. F. Curl and R. E. Smalley, *Nature*, 1985, **318**, 162.
2 N. G. Szwacki, A. Sadrzadeh and B. I. Yakobson, *Phys. Rev. Lett*., 2007, **98**, 166804.
3 (a) A. Ceulemans, J. T. Muya, G. Gopakumar and M. T. Nguyen, *Chem. Phys. Lett.* 2008, **461**, 226. (b) J. T. Muya, E. Lijnen, M. T. Nguyen and A. Ceulemans, *ChemPhysChem,* 2013, **14**, 346.
4 (a) S. De, A. Willand, M. Amsler, P. Pochet, L. Genoverse and S. Grodecker, *Phys. Rev. Lett*, 2011, **106**, 225502; (b) Y. Li, G. Zhou, J. Li, B-L, Gu and W. Duan, *J. Phys. Chem. C*, 2008, **112**, 19268.
5 (a) H. T. Pham, L. V. Duong, N. M. Tam, M. P. Pham-Ho and M. T. Nguyen, *Chem. Phys. Lett.* 2014, **608**, 295. (b) H-J. Zhai, Y-F. Zhao, W-L. Li, Q, Chen, H. Bai, H-S. Hu, Z. A. Piazza, W-J. Tian, H-G. Lu, Y-B. Wu, Y-W. Mu, G-F. Wei, Z-P. Liu, J. Li, S-D. Li and L-S. Wang, *Nature Chem.*, 2014, **6**, 727
6 G. Martinez-Guajardo, J. L. Cabellos, A, Diaz-Celaya, S. Pan, R. Islas, P. K. Chattaraj, T. Heine and G. Merino, *Sci. Rep.*, 2015, **5**, 11287.
7 (a) J. Lv, Y. Wang, L. Zhu and Y. Ma, *Nanoscale*, 2014, **6**, 11692; (b) T. B. Tai and M. T. Nguyen, *Nanoscale*, 2015, **7**, 3316.

8 Q. Chen, W. L. Li, Y. F. Zhao, S. Y. Zhang, H. S. Hu, H. Bai, H. R. Li, W. J. Tian, H. G. Lu, H. J. Zhai, S. D. Li and L. S. Wang, *ACS Nano*, 2015, **9**, 754.
9 Q. Chen, S. Y. Zhang, H. Bai, W. J. Tian, T. Gao, H. R. Li, C. Q. Miao, Y. W. Mu, H. G. Lu, H. J. Zhai and S. D. Li, *Angew. Chem. Int. Ed.*, 2015, **54**, 8160.
10 T. B. Tai, L. V. Duong, H. T. Pham, D. T. T. Mai and M. T. Nguyen, *Chem. Commun*., 2014,**50**, 1558.
11 (a) T. B. Tai and M. T. Nguyen, *Chem. Commun.* 2015, **51**, 7677; (b) T. B. Tai and M. T. Nguyen, *Phys. Chem. Chem. Phys*., 2015, **17**, 13672.
12 Z. A. Piazza, H-S. Hu, W-L. Li, Y-F. Zhao, J. Li and L-S. Wang, *Nature Commun*., 2014, **5**, 3113.
13 L. Cheng, *J. Chem. Phys*., 2012, **136**, 104301
14 J. Zhao, X. Huang, R. Shi, H. Liu, Y. Su and R. B. King, *Nanoscale*, 2015, **7**, 15086
15 T. B. Tai, M. T. Nguyen, *J. Chem. Theory Comput*. 2011, **7,** 1119.
16 (a) J. P. Perdew, K. Burke and M. Ernzerhof, *Phys. Rev. Lett*., 1996, **77**, 3865; (b) J. P. Perdew, K. Burke and M. Ernzerhof, *Phys Rev Lett*., 1997, **78**, 1396; (c) J. A. Pople, *J. Chem. Phys*., 1980, **72**, 650.
17 (a) M. Rittby and R. J. Bartlett, *J. Phys. Chem*., 1988, **92**, 3033; (b) P. J. Knowles, C. Hampel and H-J. Werner, *J. Chem. Phys*., 1994, **99**, 5219.
18 M. J. Frisch *et al*., Gaussian 09, Revision C.01, Gaussian, Inc., Wallingford CT, 2009.
19 H. J. Werner, *et al*. MOLPRO 09, a package of ab initio programs, 2009.
20 L. Wang, J. Zhao, F. Li and Z. Chen, *Chem. Phys. Lett*., 2010, **501**, 16
21 F. Li, P. Jin, D. Jiang, L. Wang, S. B. Zhang, J. Zhao and Z. Chen. *J. Chem. Phys*., 2012, **136**, 074302
22 T. B. Tai, N. M. Tam and M. T. Nguyen, *Theor. Chem. Acc*., 2012, **131**, 1241
23 J. Vande Vonele, M. Krack, F. Mohamed, M. Parrinello, Y. Chassaing, J. Hutter, *Comput. Phys. Commun*., 2005, **8**, 1314.
24 W. Humphrey, A. Dalke and K. Schulten, *J. Mol. Graphics*, 1996, **14**, 33.
25 (a) T. B. Tai, D. J. Grant, M. T. Nguyen and D. A. Dixon, *J. Phys. Chem. A.*,2010, **114**, 994; (b) T. B. Tai, N. M. Tam and M. T. Nguyen, *Chem. Phys. Lett*., 2012,**530**, 71; (c) A. G. Arvanitidis, T. B. Tai, M. T. Nguyen and A. Ceulemans, *Phys. Chem. Chem. Phys*. 2014, **16**,18311; (d) T. B. Tai, A. Ceulemans and M. T. Nguyen, *Chem. Eur. J*., 2012,**18**, 4510; (e) H. T. Pham, L. V. Duong, B. Q. Pham and M. T. Nguyen, *Chem. Phys. Lett*., 2013, **557**, 32; (f) L. V. Duong, H. T. Pham, N. M. Tam and M. T. Nguyen, *Phys. Chem. Chem. Phys*, 2014, **16**, 19470
26 (a) J. Oscar, C. Jimenez-Halla, R. Islas, T. Heine and G. Merino, *Angew. Chem. Int. Ed*., 2010, **49**, 5668; (b) D. Moreno, S. Pan, L. L. Zeonjuk, R. Islas, E. Osorio, G. M. Guajardo, P. K. Chattaraj, T. Heine and G. Merino, *Chem. Commun*. 2014, **50,** 8140; (c) F. Cervantes-Navarro, G. Martinez-Guajardo, E. Osorio, D. Moreno, W. Tiznado, R. Islas, K. J. Donald amd G. Merino, *Chem. Commnun*., 2014, **50**, 10680
27 H. L. Schmider and A. D. Becke, *J. Mol. Struct. THEOCHEM* 2000, **527**, 51.
28 (a) H. Jacobsen, *Chem. Eur. J*., 2010, **16**, 976; (b) H. Jacobsen, *Dalton Trans*., 2009, 4252.
29 S. N. Steinmann, Y. Mo and C. Corminboeuf, *Phys. Chem. Chem. Phys*, 2011, **13**, 20584.
30 P. v. R. Schleyer, C. Maerker, A. Dransfeld, H. Jiao and N. J. v. E. Hommes, J. Am. Chem. Soc., 1996, 118, 6317

